Anomalous antiferromagnetic coupling in Fe/Si/Fe structures with Co "dusting"

R. R. Gareev, M. Buchmeier, M. Kiessling, G. Woltersdorf, and C. H. Back

Citation: AIP Advances **1**, 042155 (2011); doi: 10.1063/1.3665914

View online: http://dx.doi.org/10.1063/1.3665914

View Table of Contents: http://aipadvances.aip.org/resource/1/AAIDBI/v1/i4

Published by the American Institute of Physics.

Anomalous antiferromagnetic coupling in Fe/Si/Fe structures with Co "dusting"

R. R. Gareev,[1] M. Buchmeier,[2] M. Kiessling,[1] G. Woltersdorf,[1] and C. H. Back[1]

[1]*Institute for Experimental and Applied Physics, University of Regensburg, Universitaetstrasse 31, 93040 Regensburg, Germany*

[2]*Institute of Applied Physics, University of Muenster, Corrensstrasse 2-4, 48149 Muenster, Germany*

(Received 9 September 2011; accepted 10 November 2011; published online 22 November 2011)

We report on anomalous antiferromagnetic coupling in Fe/Si/Fe epitaxial structures with interfacial cobalt "dusting". Antiferromagnetic coupling exceeds 75 μJ/m^2 for a 2.0 nm-thick Si spacer and is still detectable for a 2.3 nm-thick spacer at room temperature. From room temperature to T**$\sim$150K the magnetization follows Bloch's law and the coupling shows metallic-type behaviour; for lower temperatures the coupling is of insulating type. Below T*$\sim$50K an additional magnetic signal arises and the coupling becomes metallic-type again. We relate the observed features to the formation of inter-diffused magnetic FeCo-silicides with a Curie temperature close to 50 K. [doi:10.1063/1.3665914]

Artificial exchange coupled tunnelling Si-based structures are attracting special interest due to extremely strong indirect antiferromagnetic exchange coupling (AFC), which can exceed 5 mJ/m^2 at room temperature (RT).[1] These epitaxial structures reveal a low resistance-area product ($\sim$1Ω*cm^2) as well as a small impurity-assisted resonant tunnelling magnetoresistance.[2] The magnitude of the AFC can be increased substantially by utilizing ultrathin metallic $Fe_{0.5}Si_{0.5}$ interface layers with the cubic B2 crystal structure thus controlling inter-diffusion and spin-polarization directly at the interfaces.[3] A promising way to regulate the interface spin-polarization in these tunnelling structures could be employing ultrathin interface "dusting" magnetic layers with a higher spin polarization compared to iron. Theoretical considerations suggest that "dusting" of iron with ultra-thin Co is a good possibility for increasing interface spin polarization.[4]

In this article we demonstrate that Co "dusting" layers modify significantly the properties of diffused interfaces and AFC in epitaxial Fe/Si/Fe structures giving rise to a substantial shift of the coupling maximum and a peculiar temperature dependence of the exchange coupling. We relate these experimental findings to the formation of interface Fe-Co silicides with a magnetic phase transition temperature T*$\sim$50 K.

We prepared epitaxial Fe/Si/Fe structures on GaAs(001) substrates with a Fe (1 nm)/Ag (150 nm) buffer using thermal electron-gun evaporation following the deposition procedure described elsewhere.[1–3] We studied a Fe (3 nm) /Co (0.2 nm)/Si spacer/Co (0.2 nm)/Fe (5nm) /Au (cap layer) wedge-type sample with the thickness of the Si spacer t varying from 1.0 nm to 2.3 nm (sample A) as well as a sample with the same nominal thicknesses of magnetic layers but constant spacer thickness t=1.9 nm (sample B).

In order to determine the evolution of AFC with the spacer thickness we performed a detailed analysis of the exchange coupling by dynamic and static magnetization measurements at room temperature (RT). We studied AFC at RT for sample A using vector network analyzer ferromagnetic resonance (VNA-FMR). Here, the sample is placed on a coplanar waveguide and the spin-wave excitations lead to a microwave absorption signal, which can be traced as a function of frequency at a fixed in-plane biasing magnetic field.[5] The magnitude of AFC was extracted by fitting the

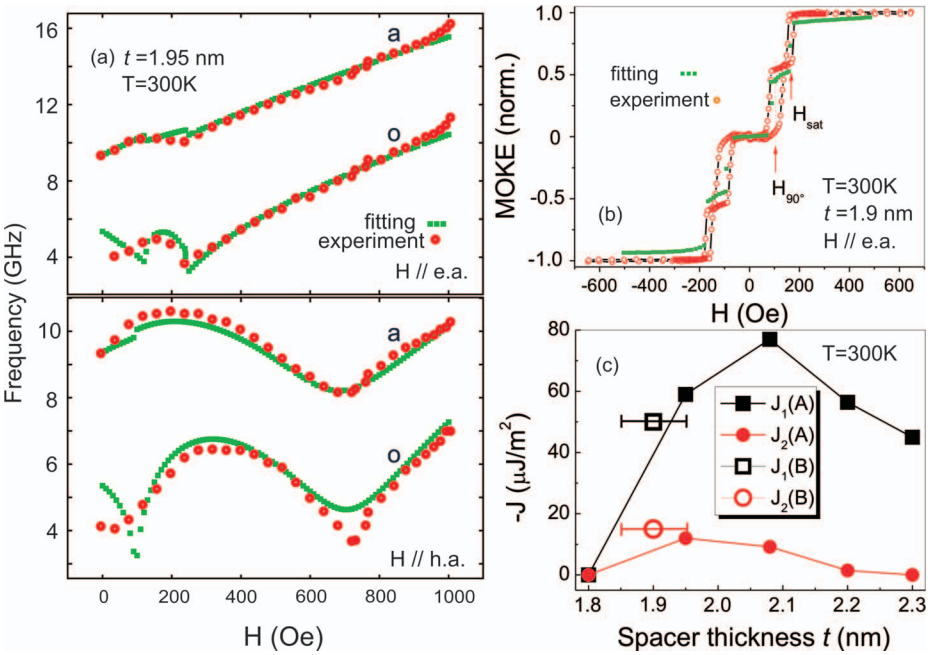

FIG. 1. Bilinear J_1 and biquadratic J_2 coupling at RT for samples A and B: (a). Typical RT experimental (open circles) and fitted (dash lines) field dependences for the frequencies of optical (o) and acoustic (o) modes of sample A for spacer thickness t=1.95 nm for H// [110] easy axis (e.a.) and [100] hard axis (h.a.), with the coupling terms J_1 = -59 μJ/m^2; J_2 = -11 μJ/m^2 corresponding to layer magnetizations M_1 = 1.5 MA/m, M_2 = 1.1 MA/m, magnetocrystalline anisotropy Kc_1 = 35 kJ/m^2, Kc_2= 8 kJ/m^2. (b). Experimental (open circles) and fitted (dash lines) MOKE hysteresis loops taken along an easy axis at RT for sample B. Coupling terms J_1= -50 μJ/m^2 and J_2 = -15 μJ/m^2 are extracted from fitting of easy and hard axes MOKE hysteresis loops with M_1=1.49 MA/m; M_2=1.45 MA/m; $2Kc_1/M_1$=38.2 mT; $2Kc_2/M_2$=50.2 mT. Arrows indicate the positions of the characteristic switching fields $H_{90°}$ and H_{sat}. (c). Exchange coupling J_1 and J_2 *versus* Si spacer thickness t for sample A extracted from fitting of experimental field dependences of spin-wave modes at RT. The open square and the open circle correspond to J_1 and J_2 extracted from the MOKE hysteresis loops of sample B.

frequency dependence of the acoustic and optic modes in the transmission spectra (sample A) as well as from the static longitudinal magneto-optical Kerr effect (MOKE) hysteresis loops (sample B) with magnetic fields applied along the easy and hard axes (see FIG. 1) by utilizing the formalism of total magnetic energy minimization as described in detail in Ref. 6. Compared to decoupled structures the total magnetic energy density in coupled systems contains additional interlayer coupling terms $J_1{*}\cos\Delta\varphi+J_2{*}\cos^2\Delta\varphi$, where $\Delta\varphi$ denotes the angle between the magnetization directions of the adjacent magnetic layers and J_1, J_2 describe bilinear (φ=180°) and biquadratic (φ=90°) coupling, respectively. FIG. 1(a) shows typical experimental and fitted field dependence of the resonance position of the optic and acoustic modes for the spacer thickness t=1.95 nm with bilinear J_1 and biquadratic J_2 exchange coupling terms determined from the fitting procedure. A typical experimental and fitted RT MOKE hysteresis loop for sample B is shown in FIG. 1(b). In FIG. 1(c) the dependence of the bilinear J_1 and biquadratic J_2 coupling terms on the spacer thickness t derived from VNA-FMR and static MOKE hysteresis is demonstrated. It is seen that static and dynamic magnetization measurements are in reasonable agreement. For sample A the AFC reaches a maximum with J_1= - 77 μJ/m^2 (J_2= - 9 μJ/m^2) for a 2.05 nm-thick Si spacer and decays rapidly with spacer thickness t but is still detectable at 2.3 nm. For t <1.8 nm coupling becomes ferromagnetic (FM) most probably due to direct FM exchange across pinholes. We note that for pure Si spacers inter-diffusion leads to FM coupling only for t<0.8 nm[1]. This shift of 1 nm to thicker spacers for samples with Co "dusting" indicates an increased inter-diffusion compared to pure Si spacers.

In FIG. 2 we present the analysis of the magnetic moment m *versus* temperature T measured using a superconducting quantum interference device (SQUID) for sample B in the saturated

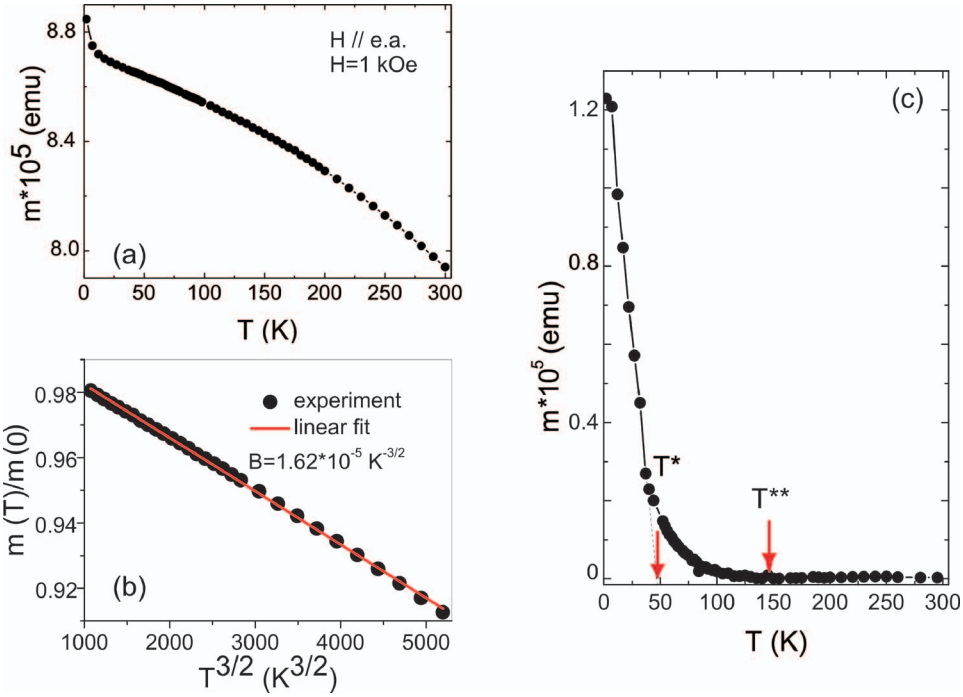

FIG. 2. SQUID magnetometer data for sample B measured in a magnetic field H=1kOe aligned along the easy axis corresponding to a parallel arrangement of the magnetic moments: (a). Magnetic moment m *versus* temperature T. (b). Experimental $m(T^{3/2})$ dependence (filled circles) and fit (line) using Bloch`s law: $m(T) = m(0)*(1-B*T^{3/2})$ corresponding to a spin-wave parameter $B=1.62*10^5$ $K^{-3/2}$. (c). Magnetic moment *versus* T for the low-temperature magnetic phase. Arrows indicate the Curie temperature T* and a characteristic temperature T** at which the deviations from Bloch`s law arise.

state (parallel alignment of magnetizations). We find that the m (T) dependence has a peculiar increase of m at low temperatures (FIG. 2(a)). For this sample with a constant spacer thickness t=1.9 nm (close to the AFC maximum) in the range of temperatures from RT to T**∼150 K the magnetic moment follows the Bloch´s law characteristic for thermal magnons with the spin-wave parameter $B=1.62*10^{-5}$ $K^{-3/2}$ (FIG. 2(b) and 2(c)). This value is close to the spin-wave parameter $B\sim1*10^{-5}$ $K^{-3/2}$ for epitaxial ultra thin iron films.[7] These findings indicate that in this range of temperatures the magnetic signal originates mostly from epitaxial iron. Close to T** the magnetic moment begins to deviate from Bloch`s law and, finally, for T*∼50K an additional magnetic signal develops. The extracted additional magnetic moment is shown in FIG. 2(c). It is seen that an additional magnetic phase with the Curie temperature T* develops. We observe a residual magnetization in region between T* and T**, which we connect with the local magnetic ordering of this additional phase. Finally, above T** the signal from additional magnetic phase vanishes and magnetization behaviour is determined by epitaxial iron layers. Thus, we established three regions of temperatures with different behaviour of magnetization caused by formation of additional low-temperature magnetic phase.

Our MOKE hysteresis data (FIG. 3(a)) show that in region 1 (above T∼75 K at which H_{sat} jumps) H_2 (in this region corresponds to H_{sat}) increases with decreasing temperature (FIG. 3(b)). In contrast, in the range of temperatures between T* and T∼75 K H_2 decreases and, finally, below T* where H_2 corresponds to H_{sat} again, H_2 increases with decreasing temperature but with a higher temperature coefficient dH_2/dT compared to region 1. In contrast, the switching field H_{90° gradually increases with temperature. Similar to the magnetization versus T data, we find three regions of temperatures with different behaviour of the switching fields between two stable magnetic states. The switching fields H_{90° and H_2 correspond to transitions from the antiparallel to the 90° alignment and from the 90°- alignment to the parallel alignment of magnetic moments, respectively. For the easy axis MOKE hysteresis loops of this sample we observe a negligible remanent magnetization

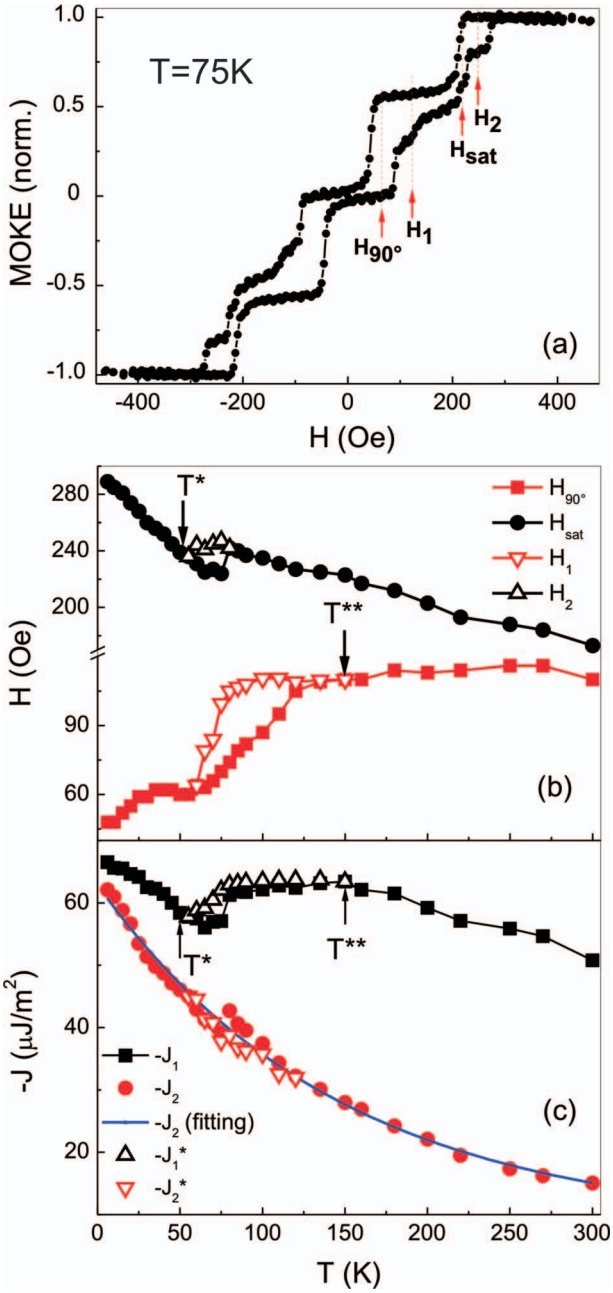

FIG. 3. The temperature dependence of the exchange coupling extracted from the longitudinal MOKE hysteresis loops for sample B: (a). A typical experimental MOKE hysteresis loop for H//[110] easy axis at T=75K (region 2). Arrows indicate the positions of the characteristic switching fields H_{90°, H_{sat} and additional switching fields H_1 and H_2. (b). Temperature dependence of the characteristic switching fields H_{90° (squares), H_{sat} (circles), H_1 (up triangles) and H_2 (down triangles). Arrows indicate characteristic temperatures T* and T**. (c). Analytically extracted J_1 and J_2 values *versus* temperature from the easy axis MOKE hysteresis loops using equations:[11] $J_1 = -(H_{sat}+H_{90^\circ})/(2d*M(T))$, $J_2 = -(H_{sat}-H_{90^\circ})/(2d*M(T))$, $J_1* = -(H_2+H_1)//(2d*M(T))$, $J_2* = -(H_2-H_1)//(2d*M(T))$, which is relevant for $K_c d > /J_1/, /J_2/, /J_1^{*}/, /J_2^{*}/$; ($K_c$ is the constant of magnetocrystalline anisotropy, d=3 nm is the thickness of the switching layer). In correspondence with the MOKE data equal magnetizations M of the magnetic layers are assumed. The line corresponds to fitting of J_2 by an exponential decay: $-J_2 = -8.1-54.9*\exp(-6.9*10^{-3}\ T)$).

for the antiparallel alignment, in spite of different nominal thicknesses of iron layers (see FIG. 1(b) and FIG. 3(a)). This is an indication that the inter-diffusion is asymmetric, it prevails at the upper interface giving rise to practically equal magnetic moments of the two iron layers for sample B. These findings are in accordance with previous studies of inter-diffused iron–silicides, which demonstrated an asymmetric diffusion profile and preferable formation of magnetic iron-silicides of a thickness near 2 nm at the upper interface (Fe on Si).[8]

Bilinear coupling is of metallic type (the coupling strength decreases with temperature) for regions 1 and 3 and shows an insulating-type behaviour for region 2, where the absolute value of J_1 increases with temperature (FIG. 3(c)). A metallic-type J_1 is a characteristic feature for Fe/Si/Fe structures where the coupling is dominated by resonant tunnelling across impurities.[2,9] The biquadratic coupling is comparable to the bilinear one and follows an exponential decrease with increasing temperature, thus favouring an extrinsic "loose-spin" mechanism of the biquadratic coupling.[10,11]

We relate the observed anomalous features to the formation of interfacial magnetic iron-cobalt silicides with a Curie temperature close to 50 K. Actually, diffused iron-rich magnetic FeCo-silicide alloys can easily be formed at interfaces by mixing of 0.2 nm-thick cobalt and several monolayers of Fe and Si. As established, iron-rich FeCo-silicides are half-metallic and become magnetic at temperatures close or below 50 K.[12,13] Following this scenario the magnetization in region 1 originates from epitaxial iron with a reduced magnetic moment of the magnetic layers caused by a diffusive formation of interface non-magnetic FeCo silicides mainly at the upper interface. In region 2 magnetic interface FeCo-silicides are formed locally giving rise to a non-collinear magnetic alignment and a peculiar insulating-type AFC. Local magnetic ordering close to the interfaces with a non-collinear magnetization could explain anomalies near H_{90° and H_{sat} (appearance of additional switching fields H_1 and H_2) in the MOKE hysteresis as well as a tail in the residual magnetization between T* and T** (see FIG. 3(b) and FIG. 2(c)). Finally, in region 3 a continuous magnetic interface FeCo-silicide alloy emerges. This leads to an increase of the effective magnetization of the magnetic layers compared to region 1 manifested in a jump of H_{sat} and increased bilinear coupling.

The insulating-type coupling in region 2 could be connected with the suppression of the impurity-assisted resonant tunnelling caused by enhanced spin-flip scattering by local non-collinear magnetic ordering of Co-containing iron-silicides near interfaces. We note that the mechanism of the spin-flip scattering by thermal fluctuations in Co-containing half-metallic silicides with a non-collinear magnetization is described in detail in Ref. 14. For mixed resonant channels the direct tunnelling mechanism can become dominating giving rise to an insulating-type bilinear coupling with a characteristic positive temperature coefficient.[15]

In conclusion, we found the antiferromagnetic coupling in Fe/Si/Fe structures with interfacial cobalt "dusting". The antiferromagnetic coupling is reaching 75 $\mu J/m^2$ and shows unusual temperature dependence with the transition from metallic-type to insulating-type behaviour. We relate the observed features to the formation of FeCo-silicides with the Curie temperature close to 50 K. A specific behaviour of the magnetization and the exchange coupling near an interfacial magnetic phase transition should be taken into account in the "dusting" interface engineering.

This work is supported by the project DFG 9209379.

[1] R. R. Gareev, D. E. Bürgler, M. Buchmeier, R. Schreiber, and P. Grünberg, J. Magn. Magn. Mater. **240**, 235 (2002).
[2] R. R. Gareev, M. Weides, R. Schreiber, and U. Poppe, Appl. Phys. Lett. **88**, 172105 (2006).
[3] R. R. Gareev, D. E. Bürgler, M. Buchmeier, R. Schreiber, and P. Grünberg, Appl. Phys. Lett. **81**, 1264 (2002).
[4] Y. Wang, X. F. Han, and X.-G. Zhang, Appl. Phys. Lett. **93**, 172501 (2008).
[5] I. Neudecker, G. Woltersdorf, B. Heinrich, T. Okuno, G. Gubbiotti, and C. H. Back, J. Magn. Magn. Mater. **307**, 148 (2006).
[6] M. Buchmeier, B. K. Kuanr, R. R. Gareev, D. E. Bürgler, and P. Grünberg, Phys. Rev. B **67**, 184404 (2001); S. M. Rezende, C. Chesman, M. A. Lucena, A. Azevedo, F. M. de Aguiar, and S. S. P. Parkin, J. Appl. Phys. **84**, 958 (1998).
[7] W. Kipferl, M. Dumm, M. Rahm, and G. Bayreuther, J. Appl. Phys. **93**, 7601 (2003).
[8] A. Gupta, D. Kumar, and V. Phatak, Phys. Rev. B **81**,155402 (2010); R. Kläsges,C. Carbone, W. Eberhardt, C. Pampuch, O. Rader, and W. Gudat, Phys. Rev. B **56**, 10801 (1997).
[9] M. Ye. Zhuravlev, E. Y. Tsymbal, and A. V. Vedyayev, Phys. Rev. Lett. **94**, 026806 (2005).

[10] J. C. Slonczewski, J. Appl. Phys. **73**, 5957 (1993).
[11] S. O. Demokritov, J. Phys. D: Appl.Phys. **31**, 925 (1998).
[12] N. Manyala, Y. Sidis, J. F. DiTusa, G. Aeppli, D. P. Young, and Z. Fisk, Nature **404**, 581 (2000).
[13] F. P. Mena, J. F. DiTusa, D. van der Marel, G. Aeppli, D. P. Young, A. Damascelli, and J. A. Mydosh, Phys. Rev.B **73**, 085205 (2006).
[14] Y. Miura, K. Abe, and M. Shirai, Phys. Rev.B **83**, 214411 (2011).
[15] P. Bruno, Phys. Rev.B **52**, 411 (1995).